Title
THREE-QUASIPARTICLE INTRUDER STATE IN Tel25 AND THE MAGNETIC MOMENT OF Sb125

Authors
Stone, N.J.
Frankel, R.B.
Shirley, D.A.

Publication Date
1967-12-01

UCRL-18000

cy. 2

University of California

Ernest O. Lawrence Radiation Laboratory

THREE-QUASIPARTICLE INTRUDER STATE IN Te^{125} AND THE MAGNETIC MOMENT OF Sb^{125}

N. J. Stone, R. B. Frankel, and D. A. Shirley

December 1967

DISCLAIMER

to be submitted to Phys. Rev.

UCRL-18000
Preprint

UNIVERSITY OF CALIFORNIA

Lawrence Radiation Laboratory
Berkeley, California

AEC Contract No. W-7405-eng-48

THREE-QUASIPARTICLE INTRUDER STATE IN Te^{125} AND THE MAGNETIC MOMENT OF Sb^{125}

N.J. Stone, R.B. Frankel, and D.A. Shirley

December 1967

THREE-QUASIPARTICLE INTRUDER STATE IN Te^{125} AND THE MAGNETIC MOMENT OF Sb^{125}*

N.J. Stone,† R.B. Frankel,‡ and D.A. Shirley

Lawrence Radiation Laboratory and Department of Chemistry
University of California
Berkeley, California

December 1967

ABSTRACT

The levels of Te^{125} have been studied using Sb^{125} nuclei, polarized at T = 0.014°K in an iron lattice, and Ge(Li) detectors. The magnetic moment of Sb^{125} was determined as 2.59 ± 0.03 nm. Levels (spins) were assigned at 35.9(3/2+), 145.4(11/2-), 322.2(9/2-), 443.7 (probably 3/2+), 462.5(5/2+), 525.4 (probably 9/2-), 636.1(7/2+), 642.3(7/2+), 671.6(5/2+). The even-parity levels could be identified with levels calculated by Kisslinger and Sorensen. Using their wave-functions we calculated E2/M1 mixing ratios and branching ratios, finding quite good agreement. The odd-parity states are of special interest. The 11/2- 145.4 keV state and 9/2- 525.4 keV state are assigned as $h_{11/2}$ quasiparticle and $h_{11/2}$ quasiparticle plus phonon. The 9/2- state at 322.2 keV is not predictable on a single-quasiparticle plus phonon theory, and is assigned as a three-quasiparticle $(h_{11/2})^3$ intruder state, bearing out Kisslinger's prediction that $(j^3)_{j-1}$ intruder states should be found in low-lying spectra for high j. Evidence for other intruder states in Rh^{100}, Ag^{109}, and Ag^{110} is given.

I. INTRODUCTION

One of the features of low temperature equilibrium nuclear orientation which has been in the past alternately a boon and a serious limitation is the fact that it is a singles measurement (requiring no coincidence between the decay products observed) that yields rather directly the angular correlation coefficients F_k. Given the range of temperatures presently available, the maximum information about the angular distribution of the decay products from oriented nuclei may be obtained by using two detectors, usually along and normal to the axis of orientation, observing in each the decay product intensity as a function of energy and specimen temperature. In practice in many cases this extreme simplicity has been lost through the failure of the detectors used, in particular NaI(Tl) γ-ray detectors, to resolve the various components of the spectrum, and as a result the technique has been inapplicable to cases involving weak or closely-spaced components in "complex" spectra.

The recent development of lithium-drifted germanium gamma-ray detectors with resolutions of about 1-3 keV and efficiencies of the order of 10^{-3} at 500 keV, has entirely changed the situation with the result that many more transitions are accessible for study by the nuclear orientation method.

Another development of importance to nuclear orientation in recent years has been the polarization of nuclei of diamagnetic atoms when present as dilute impurities in a ferromagnet.[1] The ferromagnet is cooled to temperatures of the order 0.01°K by thermal contact with a paramagnetic cooling salt which is adiabatically demagnetized from magnetic fields of order 25 kOe at 1°K.

The present work combines these two extensions to the technique to study the nuclear polarization of Sb^{125} in dilute solution in iron. In

addition spectroscopic and coincidence studies were made of the gamma transitions in the daughter Te^{125}, to check the decay scheme and assist the interpretation of the nuclear polarization data.

Sb^{125} was chosen because the difficulty of resolving various transitions in the photon spectrum has caused uncertainty in the analyses of previous spectroscopic and nuclear polarization studies using NaI(Tl) detectors. In particular a very high value of the nuclear magnetic dipole moment of Sb^{125} has been reported.[2] To improve the detailed knowledge of this system presented an excellent challenge to the high-resolution detectors.

The design of the experiment is discussed in Sec. II. The experimental results and their analysis are covered in Sec. III; the magnitude of the magnetic dipole moment of Sb^{125} is evaluated and discussed in Sec. IV. In Sec. V the spectroscopic work is described, and Sec. VI contains the conclusions for each gamma transition studied. The decay scheme is compared with theoretical calculations in Sec. VII, and an appraisal of the experiment is given in the final section.

II. EXPERIMENTAL

This project was initiated and largely completed at the Lawrence Radiation Laboratory; however, later additional nuclear orientation data have been obtained at Oxford. The two experimental systems are described separately, but the data obtained were in complete agreement and have been analysed together.

For the first work the Sb^{125} activity (a fission product) was obtained carrier-free from Oak Ridge National Laboratory. Some of the activity, in

dilute chloride solution, was placed in a small well in a 1 gm block of high purity iron and evaporated to dryness. A few microcuries of Co^{60} were also added and the well was sealed with a conical Fe plug. The block was melted at 1600°C in an argon atmosphere for about half an hour to obtain homogeneity of the Sb and Co solutes in the resulting alloy. On cooling the alloy was pounded to a flat plate which was sectioned. The activity in each section was measured to check the uniformity of the alloy. One of these sections formed the source for the polarization experiment.

The contact-cooling system comprised a tube containing finely-ground chrome potassium alum mixed to a stiff paste with a half-and-half mixture of glycerol and saturated aqueous chrome potassium alum solution. Twelve Cu fins 2 cm by 8 cm were partially embedded in the paste, giving a contact area of ~400 sq.cm. The fins were hard-soldered together at their upper ends and the solid mass was shaped as a horizontal finger which projected into a niobium cylinder. The source was soft-soldered to the underside of the finger. The tube and fin system was suspended (by nylon threads) inside a glass cryostat surrounded by liquid helium pumped to 0.97°K. Demagnetizing from fields of up to 22 kG cooled the salt to temperatures down to 0.01°K. The lowest source temperature obtained was 0.014°K. Demagnetization also left trapped flux of 2000 kG in the superconducting niobium cylinder, which served to magnetically saturate the source. The nuclear polarization axis was thus parallel to the axis of the cylinder.

Three gamma-ray detectors were used. Two of these were Ge(Li) detectors 2 cm x 3 cm with drift depths of 4 mm and 8 mm and resolution of 4 keV at 500 keV. They were used for the Sb^{125} gamma rays, and were mounted along (0°) and normal (90°) to the axis of polarization, about 4.5 cm from the source. In addition a

3" x 3" NaI(Tl) detector was used to measure the aniosotropy of the Co^{60} radiation at 0°. This (anisotropy) served as a thermometer (see Sec. V).

The high efficiency of the NaI(Tl) detector minimized the Co^{60} activity required for satisfactory temperature measurement, and thus minimized also the background under the Sb^{125} spectrum in the Ge(Li) detectors caused by the higher energy Co^{60} radiations. The intensities of all gamma rays were measured simultaneously in three 400-channel analyzers. Corrections were applied for background and the finite solid angles of the detectors.

The Oxford nuclear orientation measurements were made on an apparatus described previously.[3] The activity was obtained from the Radiochemical Centre Amersham, and source preparation was by diffusion at 900°C under a hydrogen atmosphere for 60 hours. The Ge(Li) detector used in this work, on loan from L.R.L. Berkeley, was of higher resolution (2.5 keV at 500 keV) than those used previously, allowing separate observation of all components of the spectrum.

III. RESULTS

The gamma-ray transitions in Te^{125} at 672, 636, 606, 600, 462, 426, 380, and 177 keV were observed, and all showed considerable anisotropy. Data were taken over the temperature range $20 \leq 1/T \leq 70$, concentrating on the region between 60 and 70 where the anisotropies are largest. For the most intense transition, at 426 keV, both 0° and 90° records were analyzed over the whole temperature region. A smaller Ge detector was at 90° and the data are of correspondingly poorer statistical accuracy. The results plotted as a function of 1/T are shown in Fig. 1. The temperature dependence for all transitions was the same within experimental error.

Figure 2 shows the gamma-ray spectrum above 400 keV at 1/T = 65, and at 1°K; at the latter temperature the emission is isotropic. This plot shows the clear resolution of all gamma rays except those at 600 and 606 keV. These also were resolved in the later experiments.

IV. THE MAGNETIC DIPOLE MOMENT OF Sb^{125}

The angular distribution of gamma radiation from a system of oriented nuclei is given by

$$W(\Theta) = 1 + \sum_{\nu \text{ even}} B_\nu U_\nu F_\nu P_\nu(\cos\Theta) \qquad (1)$$

where $P_\nu(\cos\Theta)$ is a Legendre polynomial, B_ν is a temperature dependent parameter describing the Boltzmann distribution among the hyperfine levels of the parent nucleus, and U_ν and F_ν are angular momentum coupling constants of unobserved and observed transitions, respectively. In the experimental temperature range only the terms for $\nu = 2,4$ need be considered.

The nuclear magnetic dipole moment is obtained from study of the ground-state transition from the 462 keV level (5/2+). This level is fed almost entirely by direct beta decay. The beta decay is allowed ℓ-forbidden with spin change of 1, i.e. a pure Gamow-Teller transition, and therefore $U_\nu F_\nu$ products can be calculated for the pure E2 transition to ground (1/2+), with no unknown beta or gamma mixing ratios (for decay scheme details see Sec. V). The values are $U_2F_2 = -0.468$, $U_4F_4 = -0.310$.

The B_ν parameters are functions of the exponent $\beta = \mu H_{eff}/IkT$ for this case of a nucleus with spin I and magnetic dipole moment μ in a ferromagnetic lattice which produces an effective magnetic field H_{eff} at the nucleus. For

Sb in Fe the magnitude H_{eff} has been measured by N.M.R. to be 230 kguass.[4] Recent measurements by beta polarization give the sign as positive.[5]

In Fig. 3 the data of W(0) for this gamma transition are compared with theoretical curves for various values of the magnetic dipole moment of Sb^{125}. Weighting the blocked points to account for their statistical errors, the final value for the moment is

$$\mu_{Sb^{125}} = \pm(2.59 \pm 0.03) \text{ nm} \qquad (2)$$

taking H_{eff} = 230 kgauss. Gamma-ray anisotropy gives only the magnitude of the product μH_{eff}, but nuclear systematics strongly indicate a positive sign for the dipole moment. This value is considerably below that obtained in a similar experiment using NaI(Tl) detectors,[2] 3.55 ±0.3 nm. The disagreement is most probably due to the inability of NaI(Tl) to resolve the 462 kdV transition from that at 426 keV, which shows a large anisotropy of the opposite sign.

The magnetic moments of nuclei having $g_{7/2}$ proton single particle ground states have been measured for several isotopes of Sb, I, and Cs. The close agreement between the present measurement of Sb^{125} and the moments of Sb^{123} (2.55 nm) and of the 7/2+ first excited state of Sb^{121} (2.51 nm)[25] are consistent with systematic observations (Fig. 4). Single-particle configuration mixing[6] predicts changes of 0.1 nm or less on addition of two neutrons, and recent calculations with the nuclear pairing force and quadrupole phonon admixture predict increases of order 0.05 nuclear magnetons.[7]

V. DECAY SCHEME OF Sb^{125}

The decay scheme of Sb^{125} has been the subject of several investigations[8-13] and although there is agreement on the main features the existence of several discrepancies and uncertainties warranted a thorough reinvestigation using Ge(Li) detectors. In addition to high resolution singles spectra, some gamma-gamma coincidence runs were made with two such detectors.

A. Gamma-Ray Energies and Intensities

Singles spectra over the whole energy range are shown in Figs. 5, 6, and 7. The gamma-ray energies and relative intensities are given in Table I. Included for comparison are the values of Narcisi[10] and Lazar.[9] The energy determinations, made using Lu^{177m}, Cs^{137}, Bi^{207}, and Ag^{110} as standards, show strong internal consistency and reveal slight errors in previous values based on conversion electron energy measurements. We thank Dr. J. Hollander and Mr. J. Haverfield for use of their efficiency calibrated detector in part of this work. We have observed new low-intensity transitions at 443.7, 407.8, and 227.5 keV, but those reported at 652, 122, 80, and 63 keV were not seen.

B. Coincidence Measurements

To check assignments of the gamma rays, fast-slow coincidence measurements were made. The counter geometry is shown inset in Fig. 9, a Pb absorber wrapped with Cd and Cu foils being used to avoid detection of backscattered photons. In the first run a gate was set on the 35.5 keV gamma ray (Fig. 8) and all coincidence pulses in a 6 sq. cm $\times$ 1-cm thick detector were recorded. The coincidence spectrum is given in Fig. 8. Observation of the transitions at 426, 600.2, and 606.4 keV are in agreement with published decay schemes; however, the 635.8 keV transition is also found with 95 $\pm$5% of its singles intensity relative to the other coincident lines. It is thus established as

originating mainly from the 671.6 keV level. The weak 407.8 keV transition is also observed.

A further run with the gate set on the combined 174 and 177-keV peak showed coincident transitions at 116(2), 172(2), 175(2), 203(2), 320(2), 426(3) and 462(4) keV (Fig. 9).

C. Nuclear Orientation

For $\mu_{Sb^{125}} = 2.59$ nm the value of B_ν for $\nu > 2$ is very small even at the lowest temperatures reached. Thus the angular distribution simplifies to $W(\theta) = 1 + B_2 U_2 F_2 P_2(\cos\theta)$. Consequently the products U_2F_2 for all the gamma rays studied are given by

$$\frac{1 - W(0)}{1 - W(0)_{462}} = \frac{(U_2F_2)}{(U_2F_2)_{462}} \qquad (3)$$

as B_2, describing orientation of the Sb^{125} parent is the same for all gamma rays. The experimental values are tabulated in Table II where they are compared with various theoretical predictions. The increased accuracy of these values compared with those given in an earlier report[14] reflects the more recent Oxford work.

D. Beta Decay

From the measured gamma-ray intensities, using the conversion coefficient measurements of Narcisi, the intensities and hence the log ft values of the various beta decay branches were calculated. The results are given in Table III.

VI. LEVEL SPINS AND PARITIES IN Te^{125}

The composite decay scheme is given in Fig. 10. In this section the data from all studies of a given level are correlated, taking into account the present work and that of other authors. Each level is discussed separately except those at 0(1/2+), 35.5 keV (3/2+), and 145.4 keV (11/2-) which are well established, and unaffected by this work.

1. 671.6 keV

The conversion coefficient of the 671.6-keV γ-ray indicates an E2 transition and thus positive parity for this state. Thus the 97-keV beta decay must be allowed (ℓ-forbidden), restricting the possible spin values to 9/2, 7/2, or 5/2. As the ground state spin is 1/2, this level is 5/2+. This assignment is consistent with the nuclear orientation result for both 671.6- and 635.8-keV transitions if the latter is mixed (see Table II). From the K conversion coefficient the higher E2 admixture is preferred. The strong line at 635 keV following Coulomb excitation[8] is also consistent. The suggestion of 3/2+ for this level[12] appears unlikely because the beta decay feed is certainly not second forbidden.

2. 642.3 keV

This level decays predominantly to the 3/2+ 35.5-keV state, with weaker transitions to the negative parity levels at 525.4 and 322.2 keV. Absence of a transition to the ground state rules out a 5/2+ assignment, which also follows from the absence of Coulomb excitation to this level. The β feed is weak. The only possible negative parity assignment consistent with no transition to the 11/2- level at 145.4 keV is 5/2-, which is not compatible with the nuclear orientation result on the 606.4-keV transition. Both nuclear

orientation and electron conversion measurements indicate 7/2+ for this level.

3. 636.1 keV

Reassignment of the 635.8-keV transition means that this level decays only to the 35.5-keV (3/2+) and 462.5- (5/2+) levels although a weak transition to the ground state is not impossible. Reassignment is based mainly on the 35.5-635.8-keV coincidence; however, additional evidence is given by the nuclear orientation result which is not compatible with a 5/2+(E2)1/2+ decay for this transition. Although the β feed log ft value is rather high for an allowed transition, the absence of decay to lower negative parity states and the sign of U_2F_2 excludes negative parity. Again nuclear orientation and electron conversion measurements are consistent with 7/2+, and 5/2+ is excluded by the failure to observe a 600-keV transition following Coulomb excitation.

4. 525.4 keV

This level decays primarily by a 380-keV transition to the 11/2- level, and is thus of negative parity. The weak first-forbidden beta feed puts an upper limit of 11/2 on the spin, and the electron conversion data give a lower limit of 7/2. The nuclear orientation result eliminates spin 7/2, leaving possible assignments 11/2- and 9/2- for this level. Both are consistent with the weak gamma feeds and decays of the level.

5. 462.5 keV

The 5/2+ spin and parity previously assigned to this level have been used in the analysis leading to the magnetic moment of Sb^{125}; the very reasonable result obtained for this moment is an indirect confirmation of the spin. The sign of the M1/E2 mixing ratio for the 426.6-keV transition from our nuclear orientation data is negative, in disagreement with angular correlation results.[12]

Recent resonance scattering cross section measurements[17] confirm our result.

6. 443.7 keV

This level has not been previously observed, but is inferred from the weak transitions at 443.7 and 407.8 keV. The 407.8-keV line is seen in coincidence with the 35.5-keV gamma ray. A weak transition at 227.5 keV feeds this level from that at 671.6 keV, and intensity calculations indicate a weak, possibly second-forbidden beta feed. The level has low spin and probably positive parity.

7. 322.2 keV

This level decays entirely to the 11/2- 145.4-keV state through a mixed M1 + E2 transition. As it is fed by a first-forbidden non-unique beta decay, and also by weak transitions from higher 7/2+ and 9/2- states the assignment for this level is 9/2-. This is consistent with nuclear orientation of the 176.8-keV gamma ray which yields (E2/M1) = -1.28 ±0.1 or -0.67 ±0.1.

8. Other Measured Parameters

Apart from the energies, spins, parities and gamma ray multipolarities listed above, measurements have also been made of the half life and magnetic dipole and electron quadrupole moment of the 35.5-keV state, 1.6 ns,[15] + 0.62 ±0.02 nm[16] and ±0.20 ±0.03 barns[17] respectively, and of the half life of the 462-keV level, $2.8 \pm 0.9 \times 10^{-11}$ sec.[18]

VII. DISCUSSION OF THE Te^{125} LEVEL SCHEME

The shell model predicts that between N = 50 and N = 82 the neutron single particle levels are $d_{5/2}$, $g_{7/2}$, $s_{1/2}$, $h_{11/2}$, and $d_{3/2}$, in order of increasing energy (ref. 7). However, the high pairing energy of the $h_{11/2}$

particles leads to the spin 1/2 ground state for N = 73, with the $h_{11/2}$ single-particle state as a low-lying isomer. The $d_{3/2}$ single particle state is also expected at low excitation energy, so that the shell model can reasonably explain the spins and parities of the first three states. The inability of the single-particle model to predict higher states or to give a quantitative explanation of the properties of the lowest states other than their spins and parities is, however, well known. Glendenning[19] has calculated the energy levels of odd-A Te and Xe isotopes, taking the interaction of the odd neutron, in single particle $s_{1/2}$ and $d_{3/2}$ states, with quadrupole vibrations of the even-even core in an intermediate coupling approximation. This approach, which necessarily gave only positive parity levels, achieved acceptable agreement with experimentally measured spins for suitably chosen single-particle energies and phonon-single particle coupling strength. However, using the same coupling strength, we have been unable to reproduce such low lying negative parity states as those found at 321 and 524 keV with any reasonable value for the $h_{11/2}$ single particle energy.

The recent calculations of Kisslinger and Sorensen[7] (hereafter referred to as K and S) using a more sophisticated form of the phonon structure, and taking into account the coupling of pairs of particles in conjugate states to form 'quasi particles', have given a set of wave functions for levels up to about 1 MeV in a wide range of basically spherical nuclei.

The general success achieved by these calculations in predicting the density and relative motion of levels is sufficiently striking to merit the comparison with experiment of their predictions of properties more sensitive to the details of the wave functions such as multipole transition rates and nuclear moments. In view of the accumulated knowledge of the level of scheme

Te^{125}, such a comparison has been made and is presented in this section.

In Table IV are given the major components of the K and S wave functions for Te^{125} below 900 keV, i.e. those with up to one phonon. Components with more than one phonon have a negligible effect on measurable quantities at these energies. Also given are the K and S energies and the energies of the experimental levels identified with the predicted ones. Figure 11 shows the two sets of levels. The energy adjustments required are of the order 0.1 to 0.2 MeV, which is within the expected accuracy of the K and S treatment. In the calculations which follow no corrections were made to the wave functions to allow for these energy changes.

We have calculated the M1 and E2 gamma ray transition probabilities using the expressions for the reduced matrix elements given by Sorensen.[29] These give T.P.(M1) = 1.76×10^{13} k E^3 sec^{-1}, where E is in MeV and the calculated B(M1) = $k(e^2\hbar^2/4m^2c^2)$, and T.P.(E2) = 1.22×10^{11} k E^5 sec^{-1}, writing B(E2) = $k \times 10^{-50}$ e^2 cm^4.

For the M1 transitions it was found that terms deriving from transitions between the single particle components of the wave functions were comparable with those corresponding to transitions between the single-particle plus phonon components. (The large reduction of T.P.(M1) for the 425-keV transition, for example, is due to cancellation between six components giving a resultant less than one tenth the sum of their moduli (see Table V)). The E2 transitions, on the other hand, are dominated by the collective de-excitations (single particle + phonon) $\rightarrow$ single particle. Following Sorensen we have used $B(E2)_{0^+ \rightarrow 2^+} = 0.46 \times 10^{-48}$ e^2 cm^4 for Te^{125}, being the average of the experimental values from the neighboring even-even nuclei, Te^{124} and Te^{126}. The phase of the collective E2 terms was found by comparison with an exactly

parallel calculation on wave functions derived using the simpler model of Glendenning. In the expression for the nuclear radius, $r = R_o A^{1/3}$, the value $R_o = 1.45 \times 10^{-13}$ cm was taken.

In Table VI the values of B(M1) and B(E2) and the corresponding T.P.'s are tabulated, the transitions being grouped according to their level of origin. The consequent multipole mixing ratios are given and compared with experiment in Table VII, and the branching ratios and life times in Table VIII. At the energies considered, internal conversion has been neglected as small compared with the uncertainty of the under-lying assumptions.

The calculations for the prominent gamma rays are very encouraging. The ground state, 35.5 keV excited state doublet branching ratios and the multipole admixtures, show agreement with experiment within a factor of 2 in the matrix elements in all cases except the probably under-estimated E2 admixture to the 635-keV transition. The 462-keV level half life is also very close to that measured.

Many of the weaker transitions involve the 442-keV level, to which assignment of a K and S level of spin 3/2 was made. In view of the satisfactory agreement obtained with experiment for the 407/442-keV branching ratio and the 228- and 201-keV intensities, the detailed comparison strengthens this assignment.

Finally, although the life time of the 35.5-keV state is much shorter than the K and S prediction,[23] the measured magnetic dipole moment is in good agreement with the calculated value of 0.64 nm.

This apparent contradiction between success and failure of the theory is probably due to the greater sensitivity of transition probabilities to details of the wave functions. This arises since, whereas magnetic moments involve only diagonal matrix elements within a single state, transition

probabilities are concerned with two states. Also the moment is directly proportional to the calculated matrix element and the transition probability depends upon its square. Finally the effect of modification of the wave function from pure single particle is only to reduce the moment by about 50% in this case, whereas the pure single particle M1 transition probability is zero. A similar example is found in the configuration mixing treatment of the 21.7-keV transition and ground state magnetic moment of Eu^{151}.[24]

VIII. NEGATIVE PARITY STATES IN Te^{125}

We have already mentioned that using the simple phonon plus single particle model of Glendenning we were unable to reproduce the low-lying negative parity states observed at 321 and 524 keV. Reference to Fig. 12 shows that such states are also conspicuously absent in the K and S calculations, which give only a close multiplet of states of spins 7/2- to 15/2- at 928 keV, from the 11/2- plus phonon configuration. While the 524-keV state might be one of these, it seems very unlikely that the 321-keV state could be explained in this way.

A recent suggestion by Kisslinger[22] may resolve this problem. This considers states derived from coupling three quasi-particles in the 11/2- level, and shows that one of these, of spin 9/2, may be expected at an energy considerably lower than the (single quasi-particle plus phonon) odd parity levels, and is thus said to "intrude" among the low-lying states. Such a level would be characterised by an anomalously low M1 transition probability, as the two quasi-particle operator for M1 de-excitation is zero if the states are pure and the single quasi-particle state is at the nuclear fermi level. This prediction is sensitive to small admixtures to the states, as the M1 single

particle transition rate is much greater than the E2. The experimental mixing ratio for the 176-keV transition, (E2/M1) = -1.28 or -0.67, shows that the E2 transition is indeed strong. The comparable M1 amplitude, the weak gamma feeds to the level, and the high beta decay log ft value are all compatible with the expected admixture of the phonon single quasi particle state of the same spin. The 9/2- state at 321 keV is therefore very likely the anticipated three quasi-particle "intruder" state.

Kisslinger has noted several other examples of $(j^3)_{j-1}$ intruder states. The first excited state in V^{51} is presumably of largely $(f_{7/2}^3)_{5/2}$ character: the large E2 admixture in the 325-keV transition to ground is a consequence of suppression of the M1 component by the seniority selection rule. Low-lying 7/2+ isomers in Ag^{107} and Ag^{109} are considered to arise from the $g_{9/2}$ proton shell and to have $\left[(9/2)^3\right]_{7/2}$ character. Confirmation of this is given by the recently measured magnetic moment of the 7/2+ 88- keV level in Ag^{109} [26], $\mu = 4.31 \pm 0.04$ nm. Before comparing this with theory we state an easily-proved theorem:

> For a configuration of n identical nucleons in j-j coupling, the g factor of any state $(j^n)_j$ is exactly that of a single nucleon.

This theorem provides a second diagnostic requirement for Kisslinger's three-quasiparticle intruder states:

1. For a nucleus with Fermi surface in a j shell the intruder state has spin j-1.
2. Its g factor is just g_j.

Six g factors in the range $1.23 \leq g \leq 1.37$ have been reported for the $g_{9/2}$ proton shell.[27] A value of 1.25 has been suggested for silver isotopes.[27]

For Ag^{109} the experimental value g = 4.31/3.5 = 1.23 is in excellent agreement, and thereby identifies this state as a three-quasiparticle intruder.

Two recently-reported magnetic moments in odd-odd nuclei with open $g_{9/2}$ proton shells also suggest three-quasiparticle character in the proton configurations. In the 74.8-keV state of Rh^{100}, most of the observed g-factor of 2.151 ±0.004[27,28] must arise from the proton configuration. If the proton configuration is coupled to spin 7/2, and the neutron configuration has g = 0.3 and is coupled to spin 3/2,[27] we have

$$g_p = \frac{2}{3} [2.151 - 0.15] = +1.33 \qquad (4)$$

which is the observed range for $g_{9/2}$ proton states. If the proton configuration were in a single-quasiparticle $g_{9/2}$ state and coupled to a spin 5/2, g = -0.3 neutron state, we would have

$$g_p = \frac{6}{11} [2.151 - 0.25] = +1.03 , \qquad (5)$$

far below the $g_{9/2}$ range. A three-quasiparticle proton configuration for the 74.8-keV state in Rh^{100} is thus strongly suggested. We note that the strength of this conclusion derives not only from the numerical agreement per se, but particularly from the fact that the very large g factor of the proton configuration, while in the range of values expected for a $(g_{9/2}^{3})_{7/2}$ state, is much larger than the values expected for other reasonable proton configurations.

The 6+ isomer of Ag^{110} provides a similar example. Using the most accurate value of μ = +3.587 nm for this state,[29] we may derive from a

discussion given previously[30]

$$g_p = \frac{2}{7} [3.587 + 0.80] = 1.25 \qquad (6)$$

for a three-quasiparticle $(9/2)^3_{7/2}$ proton state, or

$$g_p = \frac{7}{29} [3.587 + 0.59] = 1.01 \qquad (7)$$

for a single quasiparticle $g_{9/2}$ state. Only the former is in the acceptable $g_{9/2}$ range. Thus the 'intruder' state is again clearly preferred.

These results are summarized in Table IX. We interpret the observed g factors, together with the other evidence cited above as demonstrating conclusively that three-quasiparticle intruder states are indeed observed over a wide range of isotopes as Kisslinger has predicted.

IX. CONCLUSION

This experiment shows the very considerable potential of the low temperature nuclear orientation technique, allied to high resolution gamma spectroscopy, in elucidation the details of complex decay schemes. Comparison of experiment with the calculations of Kisslinger and Sorensen has shown the considerable degree of detailed success of the theory, for positive parity states, and revealed the less satisfactory way in which they describe the negative parity states. The low lying 9/2- state has been shown to be of strong theoretical interest.

ACKNOWLEDGMENTS

The authors would like to thank Dr. N. K. Glendenning and Dr. L. S. Kisslinger for their help and discussions on the theoretical aspects of this work, and Dr. M. Sott, Mr. J. J. Huntzicker, and Mr. P. G. E. Reid for help in various parts of the nuclear orientation experiment. We also acknowledge the loan of the high resolution Ge(Li) detector to the Oxford Nuclear Orientation group by L.R.L. Berkeley during sabbatical leave by one of us (D.A.S.).

ADDENDUM

Since this paper was written, the decay scheme study of Mazets and Sergeenkov has been published,[31] and is in full agreement with the conclusions given here. Also the nuclear orientation/nuclear magnetic resonance technique has been applied to Sb^{125},[32] yielding the moment value $M_{Sb^{125}} = 2.62 \pm 0.06$ nm, for $I = 7/2$, in excellent agreement with our result. This agreement confirms the spin of ^{125}Sb as 7/2.

FOOTNOTES AND REFERENCES

*This work was done under the auspices of the U. S. Atomic Energy Commission.

†Present address: Mullard Cryomagnetic Laboratory, The Clarendon Laboratory, Oxford, England.

‡Present address: The National Magnet Laboratory, Cambridge, Massachusetts.

1. B. N. Samoilov, V. V. Skylarevski, and E. P. Stepanov, Sov. Phys. J. E. T. P. 9, 972 (1959).
2. J. Hess, W. Weyhmann, B. Greenebaum, and F. M. Pipkin, Bull. Am. Phys. Soc. 9, 562 (1964).
3. I. A. Campbell, N. J. Stone, and B. G. Turrell, Proc. Roy. Soc. A283, 379 (1965).
4. M. Kontani and I. Itoh, J. Phys. Soc. Japan 22, 345 (1967).
5. B. N. Samoilov et al., in Proceedings of the Ninth International Conference on Low Temperature Physics, Columbus, Ohio, (September 1964).
6. H. Noya, A. Arima, and H. Horie, Prog. Theor. Phys. Suppl. 8, 33 (1963).
7. L. S. Kisslinger and R. A. Sorensen, Rev. Mod. Phys. 35, 853 (1963).
8. L. W. Fagg, E. A. Wolicki, R. O. Bondelid, K. L. Dunning, and S. Snyder, Phys. Rev. 100, 1299 (1955).
9. N. H. Lazar, Phys. Rev. 102, 1058 (1956).
10. R. S. Narcissi, The Radioactivity of Sb^{125} and Te^{125m} (thesis) Harvard (1959).
11. G. Chandra and V. R. Pandharipande, Nucl. Phys. 46, 119 (1963).
12. T. Mamura, T. Iwashita, Y. Skemoto, and S. Kageyama, J. Phys. Soc. Jap. 19, 239 (1964).
13. K. C. Mann, F. A. Payne, and R. P. Chaturvedi, Can. J. Phys. 42, 1700 (1964).

14. N. J. Stone, R. B. Frankel, and D. A. Shirley, University of California, Lawrence Radiation Laboratory, Nuclear Chemistry Division Annual Report, UCRL-11828, 1964.

15. R. L. Graham and R. E. Bell, Can. J. Phys. 31, 377 (1953).

16. R. B. Frankel, J. J. Huntzicker, D. A. Shirley, and N. J. Stone, to be published.

17. C. E. Violet, R. Booth, F. Wooten, Phys. Letters 5, 230 (1963).

18. F. R. Metzger and R. S. Raghaven, Phys. Rev. 145, 968 (1966).

19. N. K. Glendenning, Phys. Rev. 119, 213 (1960).

20. R. A. Sorensen, Phys. Rev. 132, 2270 (1963).

21. R. A. Sorensen, Phys. Rev. 133, B281 (1964).

22. L. S. Kisslinger, Nucl. Phys. 78, 341 (1966).

23. J. S. Geiger, R. L. Graham, J. Bergstrom, and F. Brown, Nucl. Phys. 68, 352 (1965).

24. E. E. Berlovich and G. M. Bukat, Izv. Akad, Nauk. SSSR 28, 214 (1964).

25. S. L. Ruby and G. M. Kalvius, Phys. Rev. 155, 353 (1967), and private communication.

26. G. M. Stinson and R. G. Summers-Gill, Physics in Canada 22, No. 2, 43 (1966).

27. E. Matthias, D. A. Shirley, J. J. Evans, and R. A. Naumann, Phys. Rev. 140, B264 (1965).

28. E. Matthias and D. A. Shirley, Nucl. Instr. Methods 45, 309 (1966).

29. Stephen G. Schmelling, thesis, University of California, Berkeley (1967).

30. W. C. Easley, N. Edelstein, M. P. Klein, D. A. Shirley, and H. H. Wickman, Phys. Rev. 141, 1132 (1966).

31. E. P. Mazets and Yu V. Sergeenkov, Bull. Acad. Sci. USSR Phys. Series 30, 1237 (in English).

32. J. A. Barclay, W. D. Brewer, E. Matthias, and D. A. Shirley, Proc. Int. Conf. Hyperfine Interactions Detected by Nucl. Radiations, Asilomar, 1967, to be published.

Table I. Gamma ray energies and relative intensities in the decay of Sb^{125}. Intensity measurements by Narcisi and Lazar are given in columns 3 and 4. Columns 5 and 6 show the measured K-conversion coefficients and consequent multipole assignments due to Lazar

Energy (keV)	Relative gamma intensity			K Conversion Coefficient	Multipolarity
	this work	Narcisi	Lazar		
671.6	5.9 ±5	6.1 ±1.5	-	0.0033	E2
635.8	40.9 ±4	35.7 ±2.5	23 ±2	0.0042	E2
606.4	15.6 ±2	16.8 ±1.7	88 ±9	0.0034	E2
600.2	58.3 ±6	61.7 ±3		0.0036	M1 + E2
462.5	34.7 ±3	32.5 ±2	31 ±3	0.0090	E2
443.7	1.1 ±2	-	-	-	
426.6	100	100	100	0.0112	M1(+ E2)
407.8	0.4 ±1	-	-	-	
380.0	5.0 ±5	4.0 ±8	3.8 ±8	0.0165	M1(+ E2)
320.7	1.2 ±2	2.6 ±0.9	8.8 ±2	-	
227.5	0.5 ±2	-	-	-	
208.5	0.9 ±2	1.0	-	-	
204.5	1.2 ±2	0.6	-		
176.8	30.5 ±3	22.0	19.0 ±2	0.156	M1 + E2
173.6					
116.9	1.2 ±2	1.2	1.4 ±7	-	
109.5	0.3 ±1	0.4	-	160	M4
35.9	-	21.5	-	11.4	M1

Table II. Nuclear Orientation of Sb^{125}

Eγ(keV)	Spin sequence proposed	U_2F_2(theory)	U_2F_2(expt.)	$\frac{E2}{M1}$ Mixing Ratio (δ)
672	$\frac{5^+}{2} \rightarrow \frac{1^+}{2}$	-0.47	-0.51 ± 0.09	Pure E2
636	$\frac{5^+}{2} \rightarrow \frac{1^+}{2}$	-0.47	-0.24 ± 0.02	Pure E2
	$\frac{5^+}{2} \rightarrow \frac{3^+}{2}$	—		$-(.36\ ^{+.2}_{-.3})$ or - (14 ± 2)
606	$\frac{7^+}{2} \rightarrow \frac{3^+}{2}$	-0.42 ± 0.05	-0.36 ± 0.04	Pure E2
600	$\frac{7^+}{2} \rightarrow \frac{3^+}{2}$	-0.42 ± 0.05	-0.42 ± 0.02	Pure E2
462	$\frac{5^+}{2} \rightarrow \frac{3^+}{2}$	—	+0.47 ± 0.03	Pure E2
426	$\frac{5^+}{2} \rightarrow \frac{3^+}{2}$	—	+0.91 ± 0.01	-0.95 ± 0.02 or -0.55 ± 0.02
380	$\frac{7^-}{2} \rightarrow \frac{11^-}{2}$	-0.20 ± 0.02	-0.47 ± 0.20	Pure E2
	$\frac{9^-}{2} \rightarrow \frac{11^-}{2}$	—		Negative
177	$\frac{7^-}{2} \rightarrow \frac{11^-}{2}$	-0.20 ± 0.20	-0.43 ± 0.03	Pure E2
	$\frac{9^-}{2} \rightarrow \frac{11^-}{2}$	—		-1.28 or -0.67

Table III. Beta decay of Sb^{125}. β-branch intensities calculated from gamma ray measurements.

End pt[8] Energy (keV)	% Intensity (this work)	log ft	
		this work	Narcisi[8]
619	14.4	9.6	9.5
443	9.5	9.2	9.3
324	0.3	10.2	-
302	38.5	8.0	7.9
240	1.5	9.1	9.2
131	16.8	7.2	6.9
124	5.2	7.6	7.6
112	-	-	>8.5
96	13.8	6.9	7.5

Table IV. Principal components of K and S wave functions (for detailed explanation of headings see ref. 5)

State 1^{π}	$E_{K \text{ and } S}$ (keV)	$E_{EXPT.}$ (keV)	$C_{\frac{1}{2}00}$ ‡	$C_{\frac{3}{2}00}$	$C_{\frac{5}{2}00}$	$C_{\frac{7}{2}00}$	$C_{\frac{11}{2}00}$	$C_{\frac{1}{2}12}$ †	$C_{\frac{3}{2}12}$	$C_{\frac{5}{2}12}$	$C_{\frac{7}{2}12}$	$C_{\frac{11}{2}12}$
1/2 +	0	0	.7404						.4297	..4393		
3/2 +	47	35.5		.8708				-.3199	-.1156	-.1207	.2553	
11/2 -	298	145					.9399					.1096
3/2 +	659	442		-.1481				-.4268	.7826	-.0470	-.0704	
.5/2 +	366	462			.4625			.6535	.2299	.3071	.1176	
7/2 +	424	636				.5933			.5868	-.1079	.4408	
7/2 +	834	642				-.3148			.6893	-.0072	-.4698	
5/2 +	713	671			.0339			-.3015	.8494	.0462	.1219	

Other K and S levels are $3/2^{+}$ (823 keV), $1/2^{+}$ (897), $7/2^{-}$ (928), $1/2^{-}$ (930), $9/2^{-}$ (932), $11/2^{-}$ (934), and $5/2^{-}$ (936).

‡Components of type C_{j00} represent single quasiparticles of spin j.

†Components of type C_{j12} represent quasiparticles of spin j coupled with a single quadrupole phonon to give the observed spin I of the level.

Table V. Details of the M1 Transition Probability Calculation between the $5/2^+$ level at 462 keV and the $3/2^+$ level at 35.5 keV.

5/2 level component	$C_{\frac{5}{2}}$ 00	$C_{\frac{1}{2}}$ 12	$C_{\frac{3}{2}}$ 12	$C_{\frac{5}{2}}$ 12	$C_{\frac{7}{2}}$ 12	$C_{\frac{5}{2}}$ 12	$C_{\frac{3}{2}}$ 12	Total
3/2 level component	$C_{\frac{3}{2}}$ 00	$C_{\frac{1}{2}}$ 12	$C_{\frac{3}{2}}$ 12	$C_{\frac{5}{2}}$ 12	$C_{\frac{7}{2}}$ 12	$C_{\frac{3}{2}}$ 12	$C_{\frac{5}{2}}$ 12	
Reduced matrix element in units of ($e\hbar/2mc$)	+1.89	-1.37	+0.03	-0.17	0	-0.12	+0.03	+0.29

Table VI. Calculated values of B(M1) and B(E2) and the resulting transition probabilities.

E_γ kev	B(M1) units $(e^2\hbar^2/4m^2c^2$	B(E2) units 10^{-50} e^2 cm^4	T.P. (M1) sec^{-1}	T.P. (E2) sec^{-1}
35.5	1.4×10^{-3}	2.2	1.1×10^{6}	1.4×10^{4}
442	2.3×10^{-2}	0.61	4.7×10^{10}	1.3×10^{9}
407	2.4×10^{-4}	4.4	2.9×10^{8}	5.9×10^{9}
462	-	2.4	-	6.1×10^{9}
426	3.2×10^{-3}	0.54	4.3×10^{9}	9.2×10^{8}
601	-	3.4	-	3.3×10^{10}
174	-	0.15	-	2.9×10^{6}
606	-	3.0	-	3.0×10^{10}
201	-	7.5×10^{-2}	-	3.0×10^{6}
180	1.7×10^{-2}	4.5×10^{-3}	1.7×10^{9}	1.0×10^{5}
672	-	0.42	-	7.2×10^{9}
635	7.4×10^{-3}	4.9	3.3×10^{10}	6.0×10^{10}
228	2.2×10^{-1}	0.15	2.8×10^{9}	1.1×10^{7}
209	1.3×10^{-2}	0.15	3.3×10^{10}	7.3×10^{6}

Table VII. The calculated E2/M1 mixing ratios are tabulated and compared with experiment both for amplitude and sign.

Eγ (kev)	Theory		Experiment		
	Amplitude mixing ratio E2/M1 = δ	Sign	δ	sign	
35.5	0.12	-	0.019	±	(c)
442	0.17	+			
407	4.5	+			
426	0.47	-	1.0	-	(a)
			or 0.43		
			$0.44^{+0.15}_{-0.10}$	+	(b)
180	7.7×10^{-3}	+			
636	1.35	+	0.08	-	(a)
			or 38		
228	6.3×10^{-2}	-			
209	1.5×10^{-2}	-			

[a] This work.
[b] Ref. 10.
[c] Ref. 18

Table VIII. Calculated and experimental values of level half lives and de-excitation branching ratios.

Level Energy (kev)	Half Life $\tau_{1/2}$(sec)		Eγ kev.	Relative Intensities from each level.	
	Calc.	Expt.		Calc.	Expt.
442	1.2×10^{-11}	-	442	1	1
			407	0.13	0.35
462	6.2×10^{-11}	$2.8 \pm 0.9 \times 10^{-11}$	462	1	1
			426	0.85	2.9
636	2.1×10^{-11}	-	601	1	1
			174	10^{-4}	v. small
642	$< 2.3 \times 10^{-11}$	-	606	1	1
			201	10^{-4}	not observed
			180	0.06	not observed
672	4.8×10^{-12}	-	672	0.078	0.14
			635	1	1
			228	0.030	0.013
			209	0.35	0.03

Table IX. Experimental and calculated g factors of proton configurations in one-quasiparticle and three-quasiparticle states.

Nucleus	$(1QP)^{expt}_{9/2}$	$(1QP)^{calc}_{9/2}$	$(1QP)^{expt}_{7/2}$	$(1QP)^{calc}_{7/2}$	$(3QP)^{expt}_{7/2}$	$(3QP)^{calc}_{7/2}$
Rh^{100} (74.8 keV)	1.03[a]	1.26[b]	1.33[c]	0.73	1.33[c]	1.26[b]
Ag^{109m}	-	-	1.23	0.73	1.23	1.25[b]
Ag^{110m}	1.01[a]	1.25[b]	1.25[c]	0.73	1.25[c]	1.25[b]

[a] Assuming that the proton configuration has spin 9/2.

[b] Based on empirical g-factors for $g_{9/2}$ proton states.

[c] Assuming that the proton configuration has spin 7/2.

FIGURE CAPTIONS

Fig. 1. $W(0)$ and $W(\pi/2)$ as a function of $1/T$ for the 426-keV gamma ray. Theoretical fit to the data taking $\mu_{Sb^{125}} = 2.59$ nm, $H_{eff} = 230$ koe, and $U_2F_2 = 0.91$ (see Table II).

Fig. 2. Ge(Li) spectrum of Sb^{125} above 400 keV. ——— Normal intensities, -------- Intensity at 0.014°K with source polarized.

Fig. 3. $1 - W(0)$ versus $1/T$ for the 462-keV gamma ray. Solid lines are for $\mu = 2.54$, 2.64 nm. $H_{eff} = 230$ koe.

Fig. 4. Magnetic dipole moment systematics for $g_{7/2}$ single proton nuclei.

Fig. 5. Sb^{125} singles gamma spectrum a) 50 to 275 keV.

Fig. 6. Sb^{125} singles gamma spectrum b) 250 to 480 keV.

Fig. 7. Sb^{125} singles gamma spectrum c) 430 to 680 keV.

Fig. 8. Gamma spectrum in prompt coincidence with 35.5-keV gamma ray.

Fig. 9. Ge-Ge coincidence spectrum with 174 + 177-keV gamma ray window. Inset. Detector-source geometry.

Fig. 10. Decay scheme of Sb^{125}.

Fig. 11. Energy level comparison for Te^{125} between experiment and the calculations of K and S.

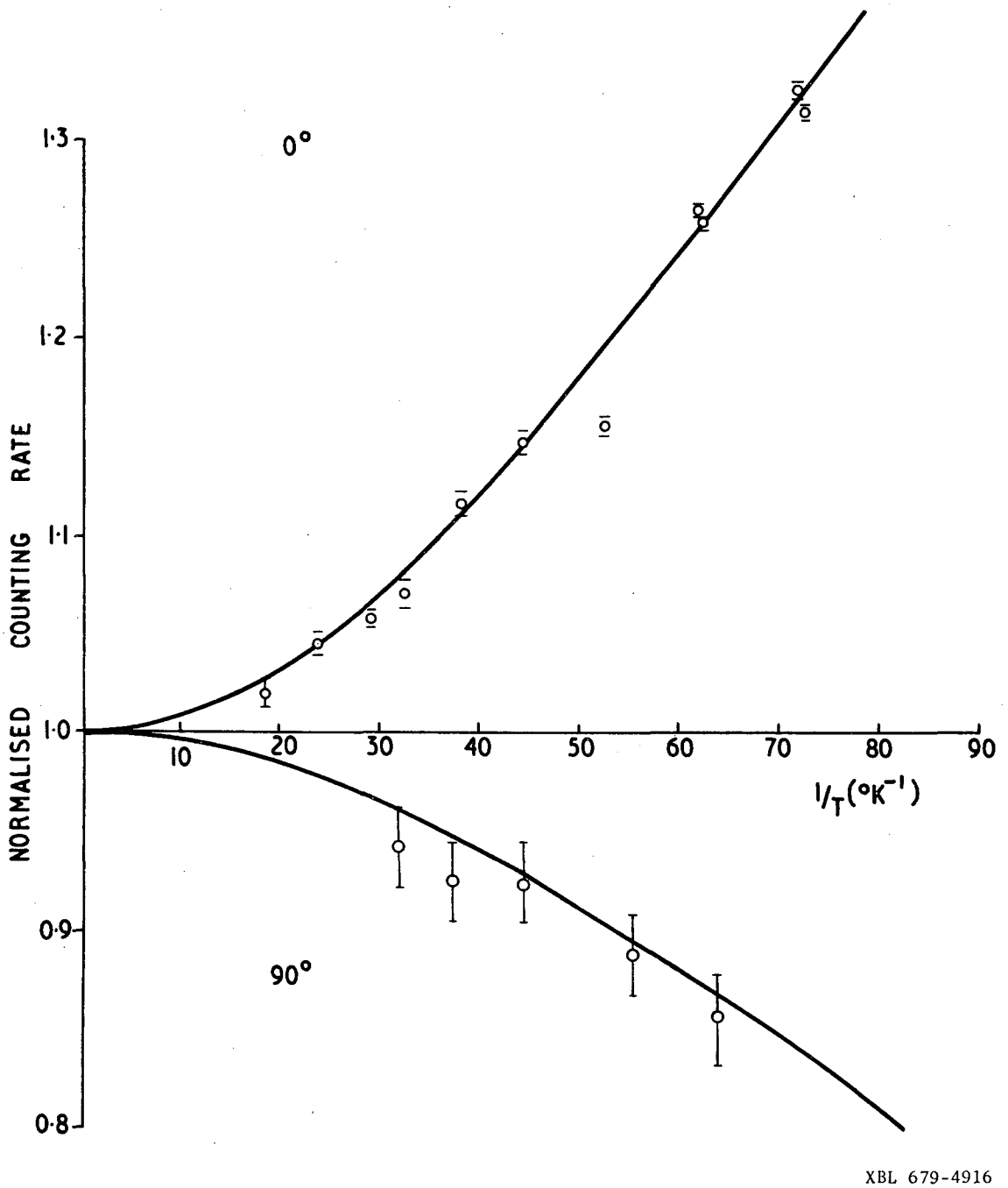
0°
90°
NORMALISED COUNTING RATE
1·3
1·2
1·1
1·0
0·9
0·8
10
20
30
40
50
60
70
80
90
1/T (°K⁻¹)
XBL 679-4916

Fig. 1

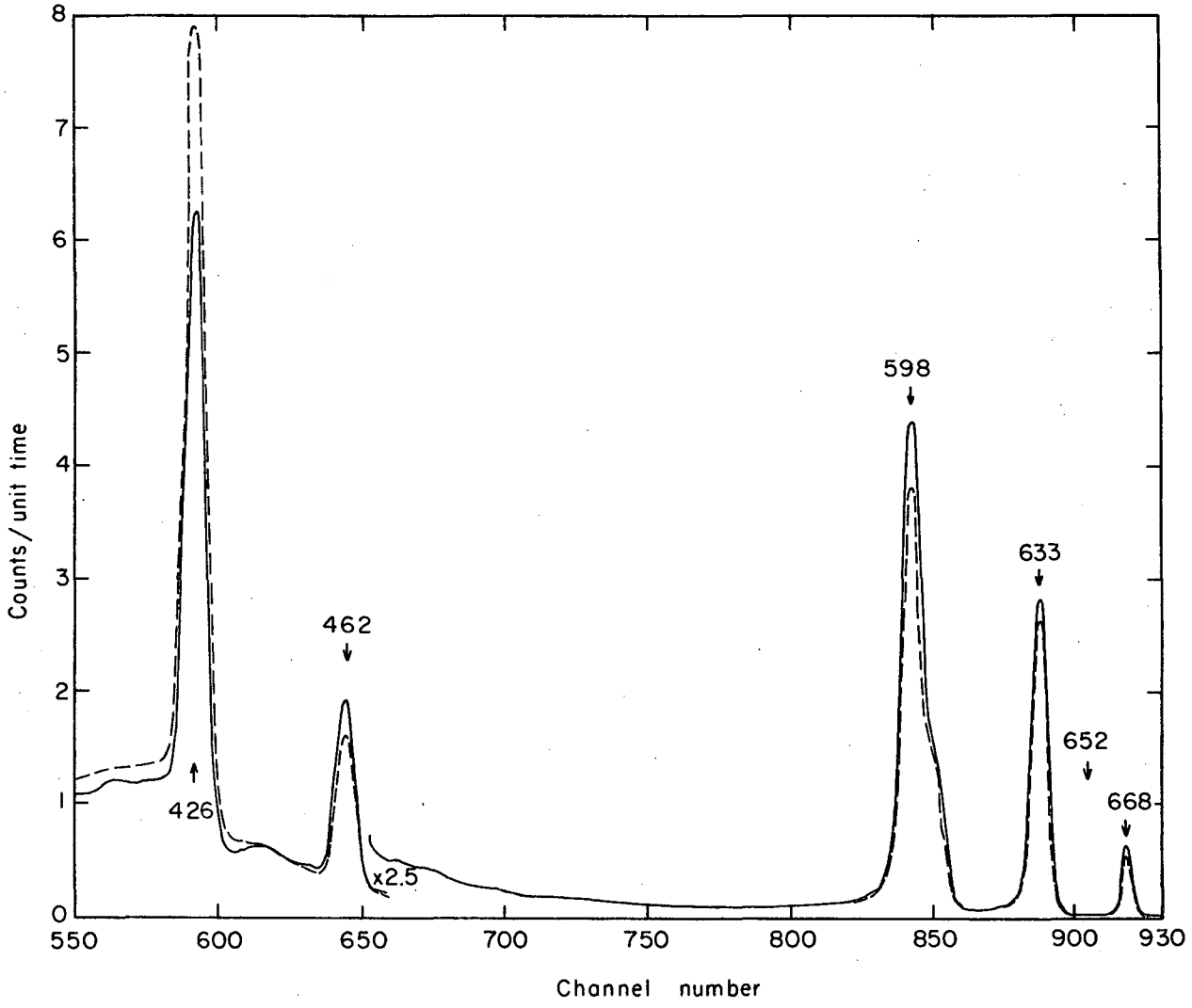
Counts / unit time
Channel number
426
462
598
633
652
668
x2.5
MUB-4851

Fig. 2

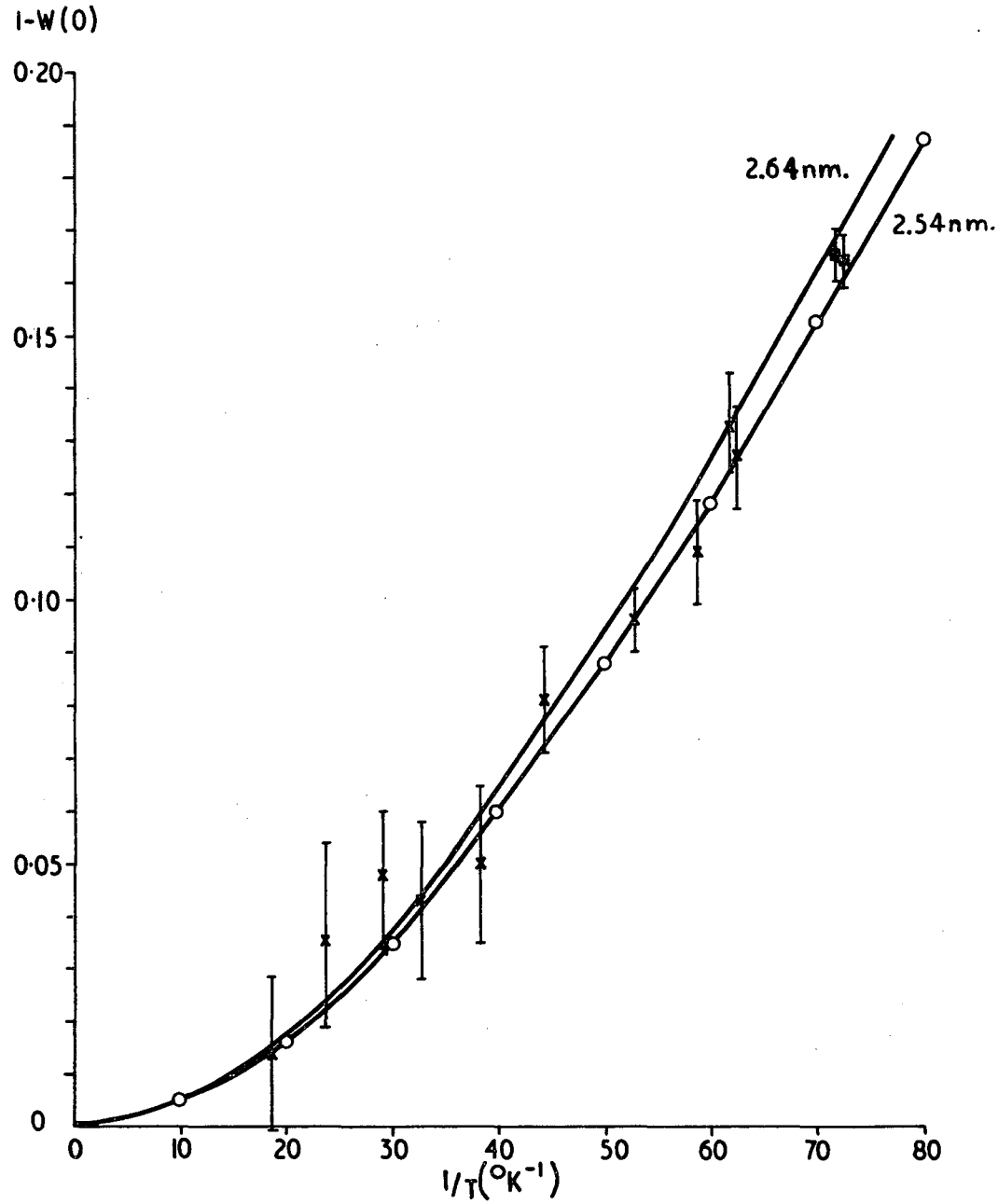
1-W(0)
0·20
0·15
0·10
0·05
0
0
10
20
30
40
50
60
70
80
1/T(°K⁻¹)
2.64nm.
2.54nm.
XBL 679-4914

Fig. 3

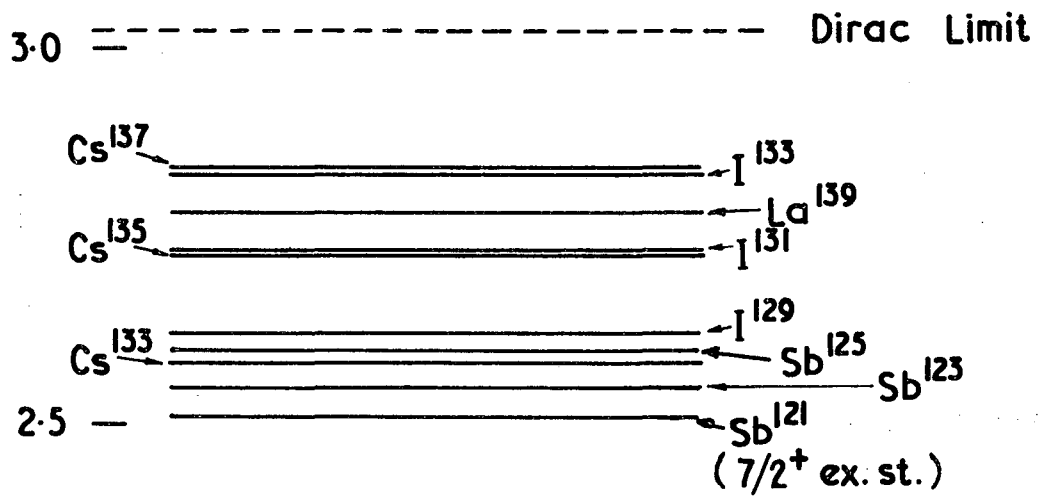

XBL 679-4915A

Fig. 4

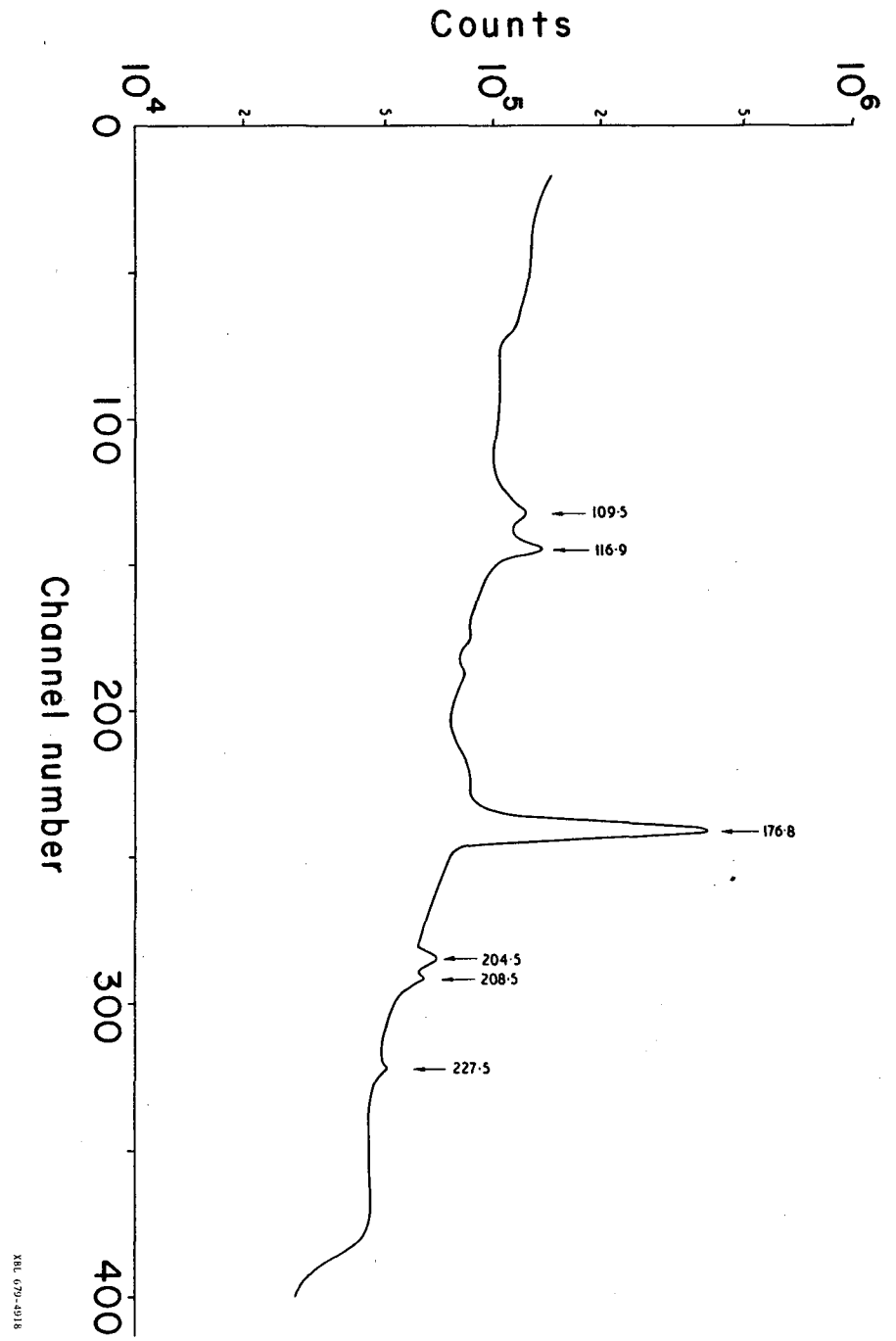
Counts
10^4
2
5
10^5
2
5
10^6
0
100
200
300
400
Channel number
109·5
116·9
176·8
204·5
208·5
227·5
XBL 679-4918

Fig. 5

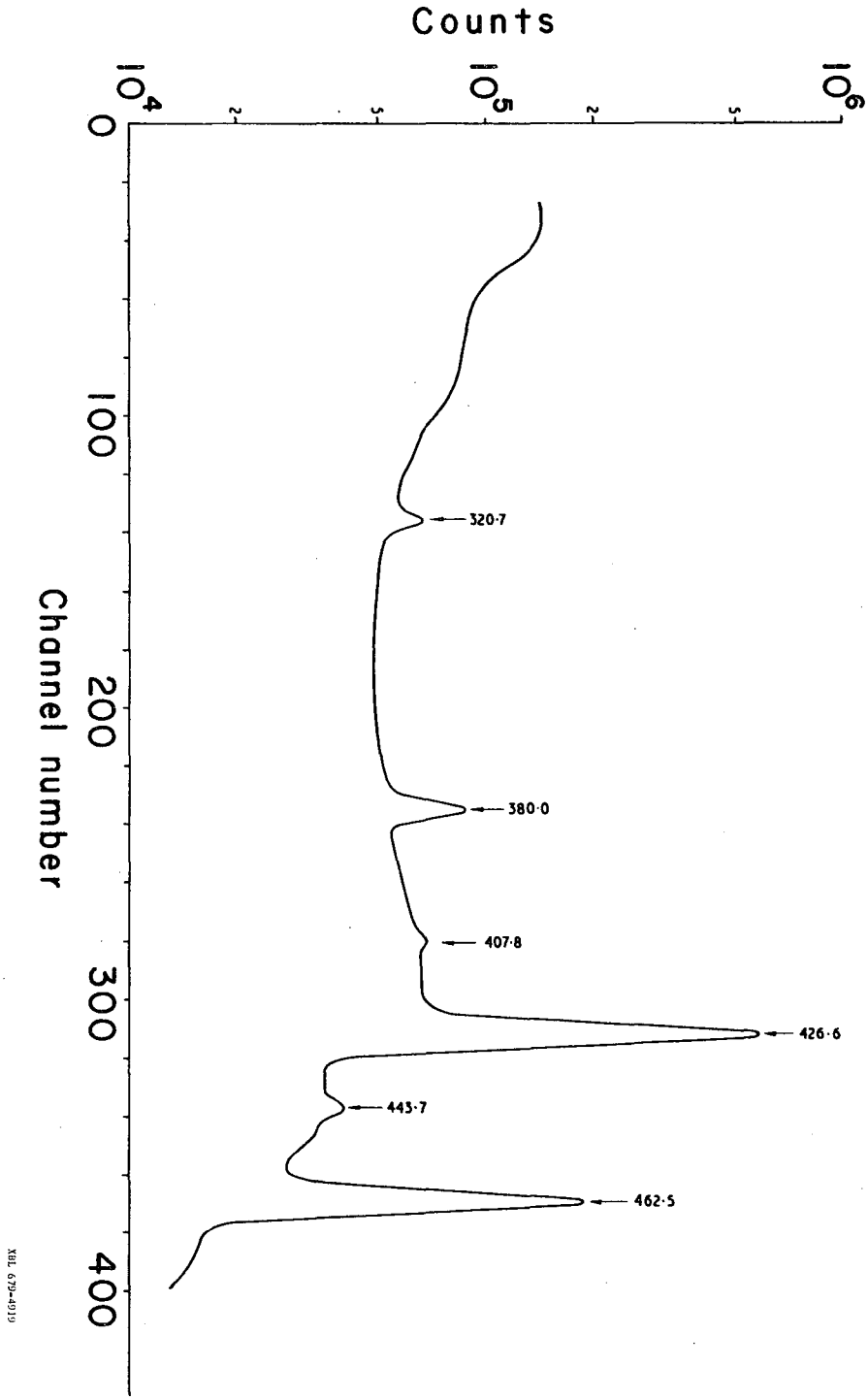
Counts
10^4
2
5
10^5
2
5
10^6
0
100
200
300
400
Channel number
320·7
380·0
407·8
426·6
445·7
462·5
XBL 699-4919

Fig. 6

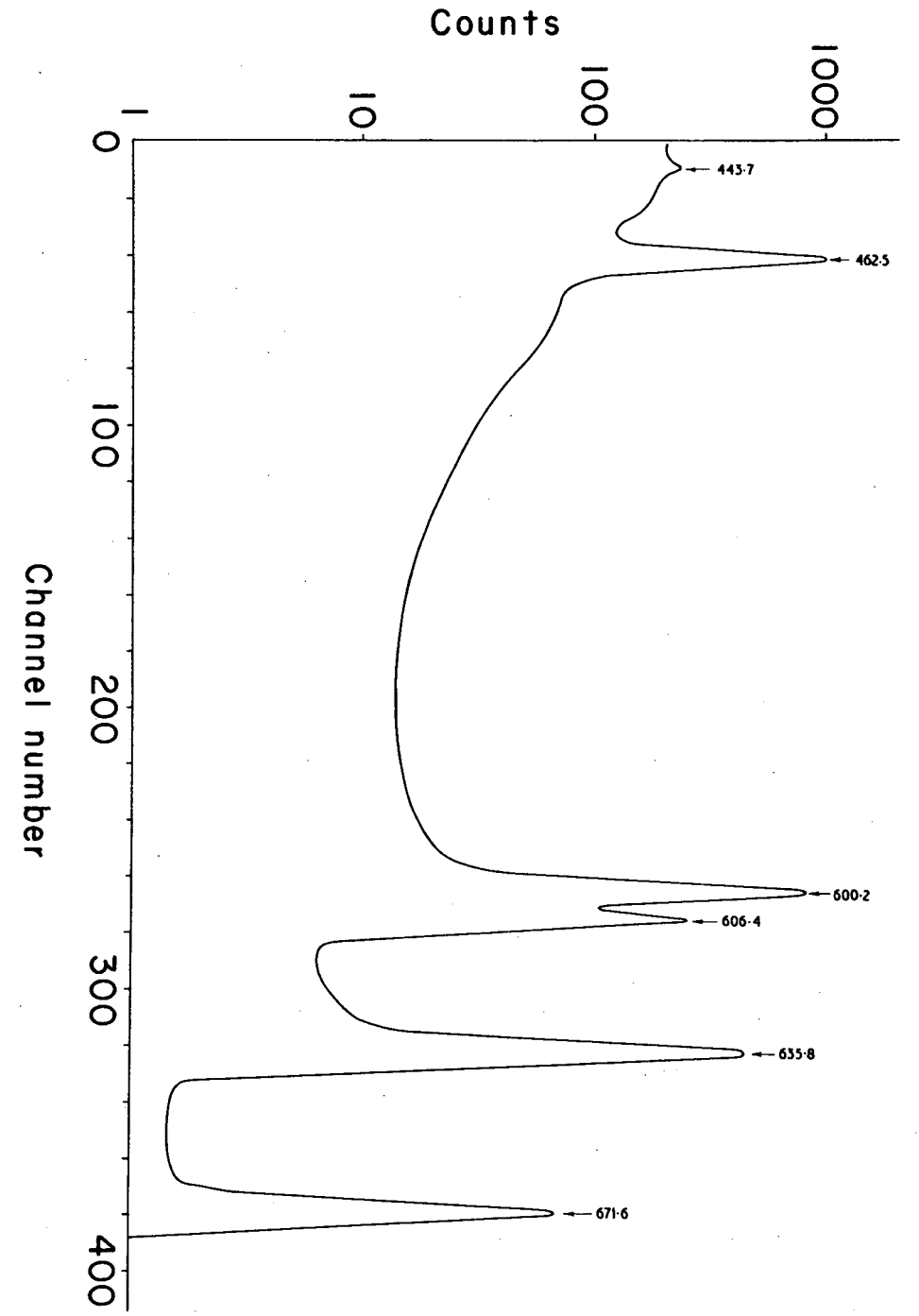
Counts
1
10
100
1000
0
100
200
300
400
Channel number
443·7
462·5
600·2
606·4
635·8
671·6
XBL 679-4920

Fig. 7

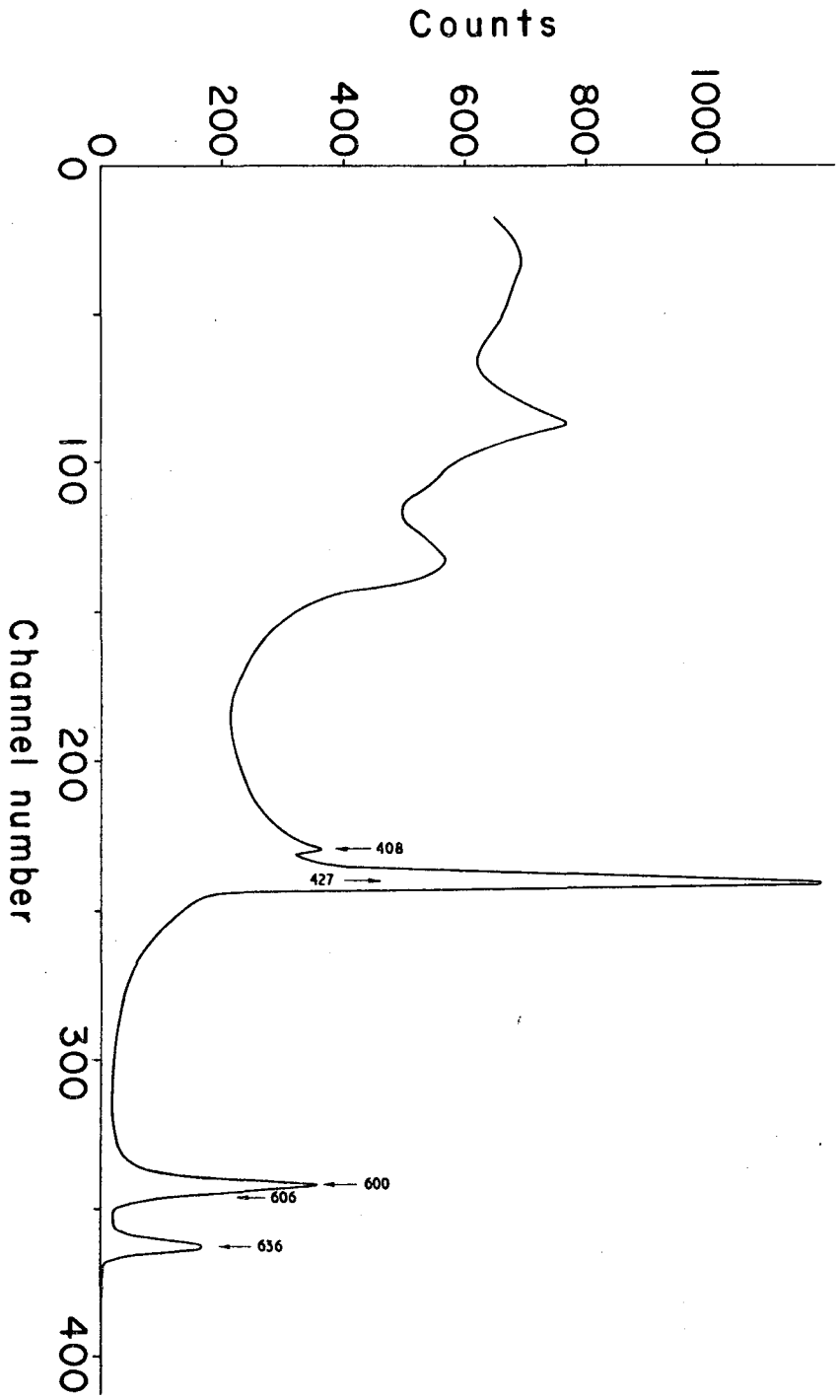
Counts
0
200
400
600
800
1000
Channel number
0
100
200
300
400
408
427
600
606
636
XBL 679-4921

Fig. 8

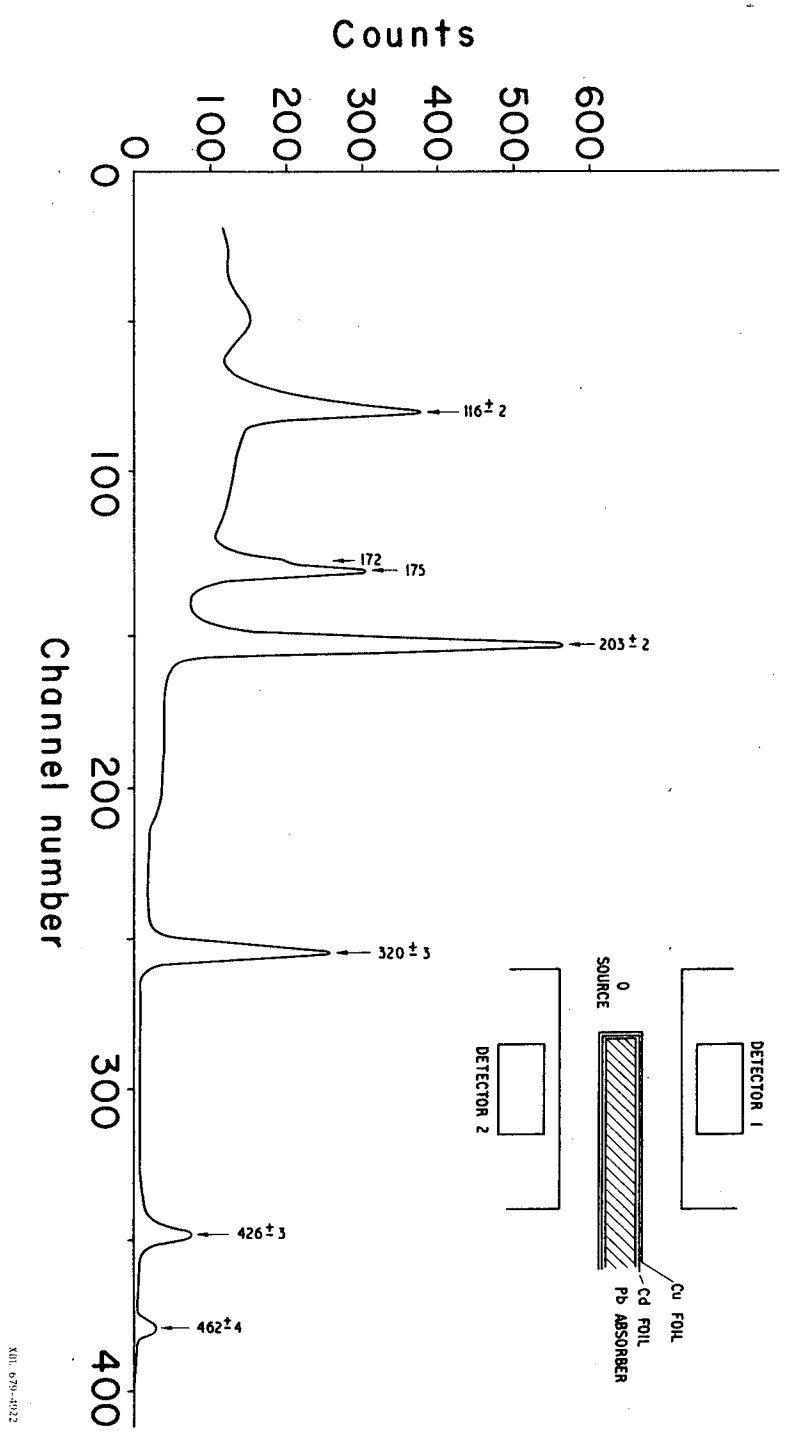
Counts
0
100
200
300
400
500
600
Channel number
0
100
200
300
400
116 ± 2
172
175
203 ± 2
320 ± 3
426 ± 3
462 ± 4
SOURCE
DETECTOR 1
DETECTOR 2
Cu FOIL
Cd FOIL
Pb ABSORBER
XBL 679-1922

Fig. 9

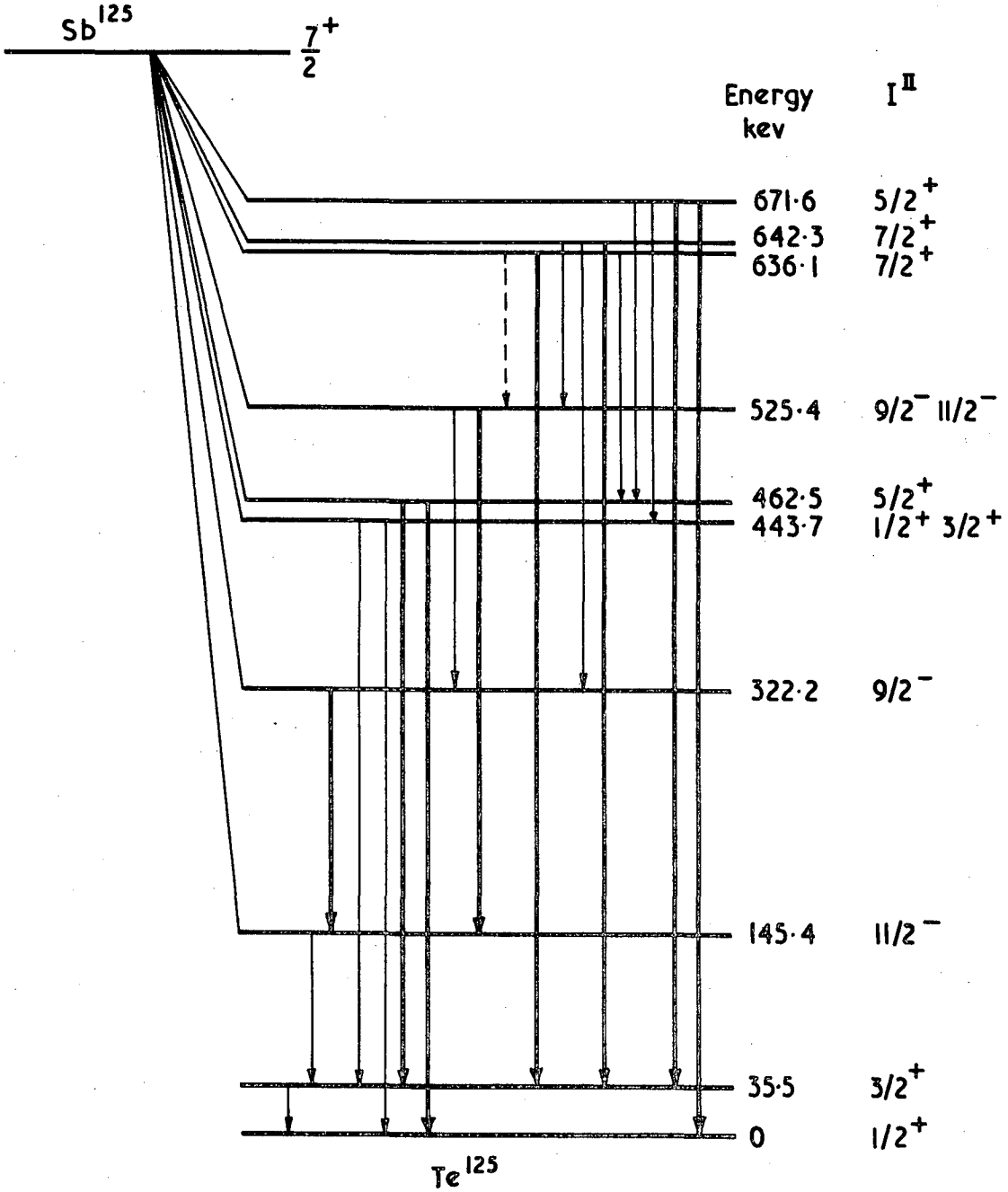

XBL 679-4917

Fig. 10

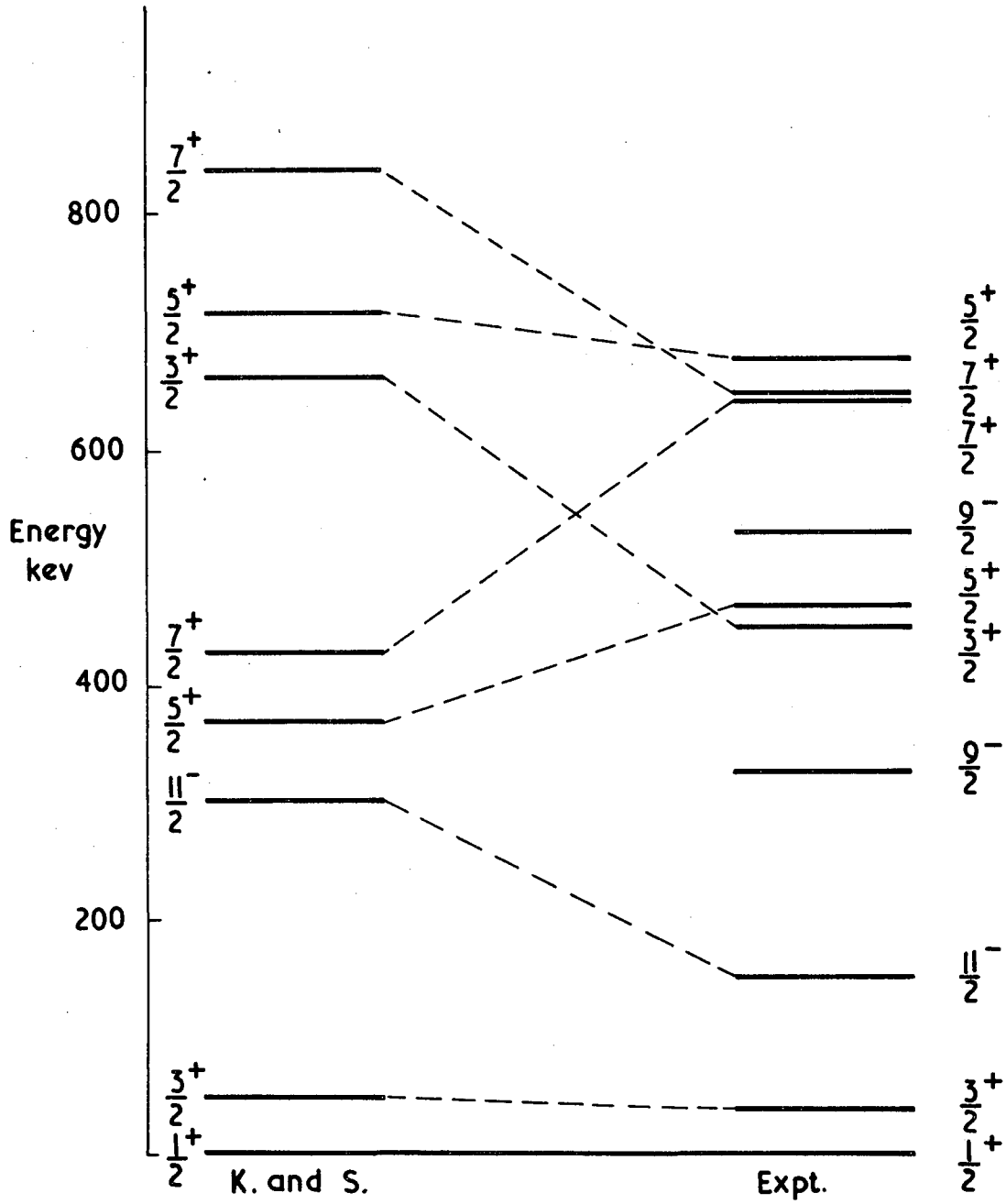

XBL 679-4913

Fig. 11